J. Fluid Mech. (1970), *vol.* 41, *part* 4, *pp.* 851–864
Printed in Great Britain

A theory for free outflow beneath radial gates

By BRUCE E. LAROCK
University of California, Davis

(Received 18 July 1969)

An analysis is made of the free outflow of fluid from those underflow gates known as radial or Tainter gates. Attention is focused on a correct treatment of the effects of gate curvature and of gravity on the flow. The rapidly convergent, iterative solution is based on the combined use of conformal mapping and the Riemann–Hilbert solution to a mixed boundary-value problem. A limited comparison with some experimental results shows agreement to be good.

1. Introduction

The radial or Tainter gate and various forms of the vertical sluice gate are both underflow gates commonly used to regulate the flow of water over spillway crests and through canals and a wide variety of other hydraulic conveyance structures. In hydrodynamics, however, past studies have almost entirely ignored the radial gate in favour of the vertical sluice gate, for the latter presents to the theoretician a far more tractable, although still difficult, analytical problem.

For nearly a century various investigators have developed analytical solutions which describe the efflux of fluid from containers of various geometries and which in varying degrees are related to the actual sluice gate problem, which in terms of two-dimensional, incompressible, inviscid flow is properly posed as a gravity-affected flow possessing two free surfaces, one upstream and one downstream of the gate. A first approximate measure of the contraction coefficient was found by analyzing the efflux from a slot in the wall of an infinite reservoir (Rayleigh 1876). Also considered by Rayleigh and successors was the effect of finite channel width on the efflux from an enclosed slot. However, these studies all neglected gravity. The next advances were made by attempting to alter the shape of the hodograph plane to account for the effect of gravity on the downstream free surface (Pajer 1937; Benjamin 1956; Perry 1957). Southwell & Vaisey (1946) applied relaxation techniques to the problem. Fangmeier & Strelkoff (1968) and Klassen (1967) present solutions to the vertical sluice gate problem, each of which avoids using the hodograph plane and instead formulates a non-linear integral equation from which the solution is deduced. Of all these solutions, only that of Fangmeier & Strelkoff is 'exact' in the sense that it alone properly accounts for the existence of both free surfaces. Even more recently the Riemann–Hilbert technique has been applied to the problem of gravity-affected flow from planar sluice gates of arbitrary inclination (Larock 1969*a*).

On the other hand, progress toward a workable analytical theory for the detailed description of flow past radial gates has been almost non-existent.

Metzler (1948) and later Toch (1955) have conducted some of the better known experimental research on the characteristics of radial gate flows. In his study, Toch correlated lip angle with von Mises's (1917) work with some success. The U.S. Army Engineer Waterways Experiment Station at Vicksburg, Mississippi, has used these and other data to prepare hydraulic design charts which are used to describe the discharge properties of these gates. More recently Babb, Moayeri & Amorocho (1966) conducted an independent experimental programme on models of the radial gates to be used as part of the California Aqueduct project.

The goal of the present work was to develop a realistic and yet workable theory for the analytical description of flow past radial or Tainter gates. This project builds on two previous studies conducted by the writer: (i) The basic flow model was developed in a study of gravity-affected flow past planar sluice gates of arbitrary inclination (Larock 1969*a*); the method of incorporating the effects of gravity into this analysis was also developed there. (ii) Work on the flow of fluid past solid curvilinear boundaries forms the basis of the current treatment of the effects of gate curvature. Some examples are presented to illustrate features and uses of the theory. Theoretical discharge coefficients are compared to experimentally determined coefficients; within the limitations of the theory, the agreement is good. In this study, however, it was economically unfeasible to generate a complete set of plots for the range of the many different geometric variables, so this was not done.

2. Problem formulation

The problem formulation and solution is chosen to take advantage of some recently developed techniques which have been applied to the solution of several related problems (Larock & Street 1967; Larock 1969*a*, *b*). These techniques adapted the Riemann–Hilbert technique to problems involving free surfaces in a transverse gravity field and the flow of fluid past curvilinear solid boundaries. Nevertheless the techniques still must be applied to a model of the exact problem rather than to the exact problem itself.

Steady, two-dimensional, irrotational flow of an incompressible, homogeneous fluid past a radial gate is studied here, as shown in figure 1, which is the physical or z plane. Viscosity and surface tension are neglected. The origin of co-ordinates $z = x + iy$ is on the channel bottom directly under point A, which is the point where the upper free surface and the gate intersect. The surface AD is physically a free surface subjected to atmospheric pressure only; for mathematical reasons this surface is assumed to be horizontal and located a distance y_1 above the channel bottom. Here y_1 and y_2 are the channel depths far upstream and downstream, respectively, and q_1 and q_2 are the corresponding uniform upstream and downstream flow speeds. This model of the physical problem appears to be reasonable for $y_1/y_2 > 3$ and becomes more accurate as y_1/y_2 increases. Segment AB is the radial gate, each point P of which has some prescribed local inclination $\beta(P)$. The flow separates smoothly from point B, and eventually the flow again becomes uniform downstream at C.

The mathematical description of this flow is found by the following approach: (i) by conformal mapping the physical plane is related to a parametric upper half-plane, called the t plane, and to the complex potential plane, called the W plane; (ii) in the half-plane a well-posed Riemann–Hilbert mixed boundary-value problem is formally solved; and (iii) the formal solution is iteratively refined until the solution for the actual gravity-affected flow has been found with acceptable accuracy. The number of needed iterations depends on both the extent with which gravity affects the flow and the amount of curvature of the gate. Normally only two or three iterations are required. Although all final results of this study are presented in real form, the use of complex-variable theory is essential to the solution.

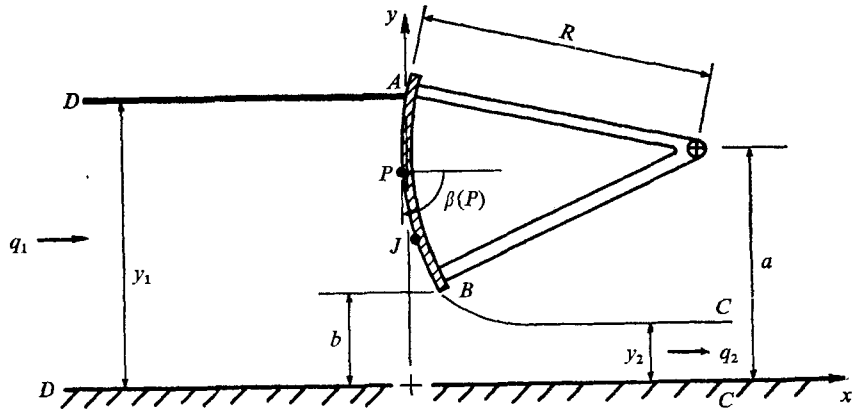

FIGURE 1. Schematic of the physical z-plane.

Mass and energy must be conserved for this flow. Mass is conserved between points C and D if

$$q_1 y_1 = q_2 y_2, \tag{1}$$

and, according to Bernoulli,

$$\frac{q_1^2}{2g} + \frac{p_1}{\rho g} + y_1 = \frac{q^2}{2g} + y = \frac{q_2^2}{2g} + y_2 \tag{2}$$

between point D, any point y on the downstream free surface, and point C, respectively, for energy conservation. Here p_1 is the gauge pressure far upstream on the upper surface, ρ is the constant fluid density, g is the gravitational acceleration, and q and y are the fluid speed and depth at the point on the free surface. To model best the upstream free surface, p_1 is equated to zero; due to the choice of flow model, however, p_1 need not necessarily be zero. Equations (1) and (2) can be arranged to give

$$\frac{q}{q_2} = \left[1 - \frac{2}{F^2}\left(\frac{y}{y_2} - 1\right)\right]^{\frac{1}{2}} \tag{3}$$

showing that the local fluid speed ratio q/q_2 is a function only of the local depth ratio and the chosen downstream reference Froude number $F^2 = q_2^2/(gy_2)$.

The downstream Froude number is a convenient measure of the effect of gravity on the flow. As (3) shows, $q \to q_2$ when F^2 becomes large, and the effect

of gravity diminishes. For all underflow gates, whether they are radial gates or planar sluice gates, the proper value of F^2 is determined by the reference depth ratio $s = y_1/y_2$ and the upstream pressure coefficient $C_{p_1} = p_1/(\frac{1}{2}\rho q_2^2)$. Specifically, (1) and (2) show

$$F^2 = \frac{2s^2(s-1)}{s^2(1-C_{p_1})-1}, \tag{4}$$

or, when $C_{p_1} = 0$ for atmospheric pressure at the upstream surface,

$$F^2 = \frac{2s^2}{s+1}. \tag{5}$$

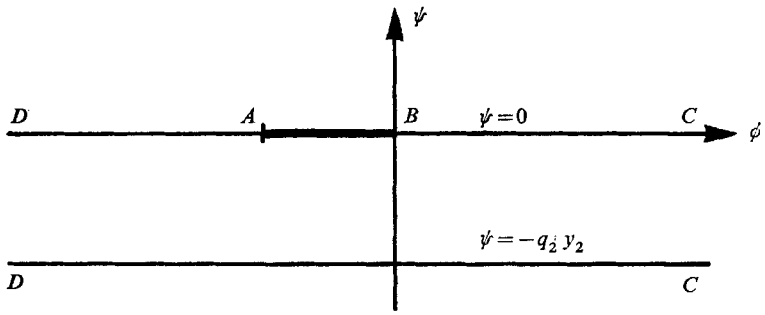

FIGURE 2. Complex potential plane $W = \phi + i\psi$.

The image of the flow in the plane of the complex potential $W = \phi + i\psi$ is an infinite slit, as shown in figure 2; ϕ is the velocity potential and ψ is the stream function with $\psi = 0$ chosen to coincide with the free surface. The W plane is related to the physical or z plane by

$$\zeta = \frac{1}{q_2}\frac{dW}{dz} = \frac{q}{q_2}e^{-i\theta}, \tag{6}$$

where ζ is the normalized complex velocity, and θ is the argument of the velocity. Using the more convenient variable

$$\omega = \ln \zeta = \ln (q/q_2) + i(-\theta), \tag{7}$$

(6) formally gives z, as a function of the one variable t, as

$$z = \frac{1}{q_2}\int e^{-\omega(t)}\frac{dW}{dt}\,dt. \tag{8}$$

To determine $W(t)$ the complex potential plane is mapped to the upper half t plane, figure 3, so that the boundaries of the flow domain map onto the real line as shown. To ensure uniqueness of the mapping (Churchill 1960), the following point correspondence is chosen:

$$\left.\begin{aligned} &B\colon W = 0, && t = 0,\\ &C\colon W \to +\infty, && t = -1,\\ &D\colon W \to -\infty, && t \to \infty. \end{aligned}\right\} \tag{9}$$

The scale constant of the mapping is found by requiring $\mathrm{Im}\,(W) = -\psi_0 = -q_2 y_2$ for real $t \leqslant -1$; thus,

$$W(t) = -\frac{q_2 y_2}{\pi} \ln (1+t). \tag{10}$$

The physical plane is then given in normalized form as

$$\frac{z}{y_2} = \frac{x+iy}{y_2} = -\frac{1}{\pi}\int e^{-\omega(t)} \frac{dt}{1+t}. \tag{11}$$

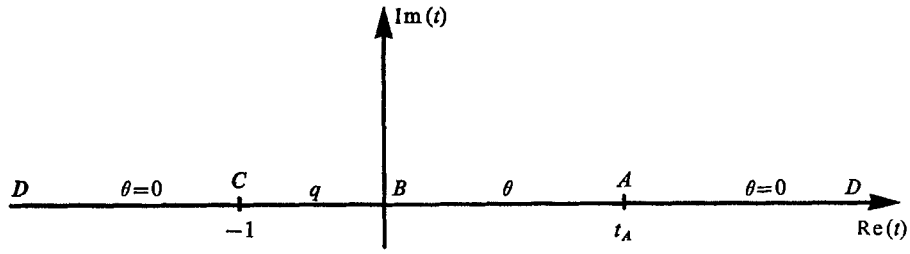

FIGURE 3. The parametric t plane.

Presuming for a moment that either the magnitude or the inclination of the complex velocity is known on the entire boundary of the flow domain, one can then convert this information into that required to solve a well-posed Riemann–Hilbert mixed boundary-value problem. For this problem one may state that

$$\left.\begin{aligned} &\mathrm{Im}\,(\omega) = 0 && (-\infty < t < -1),\\ &\mathrm{Re}\,(\omega) = \tfrac{1}{2}\ln\left[1 - \frac{2}{F^2}\left(\frac{y(t)}{y_2} - 1\right)\right] && (-1 < t < 0),\\ &\mathrm{Im}\,(\omega) = \beta(t) && (0 < t < t_A),\\ &\mathrm{Im}\,(\omega) = 0 && (t_A < t < \infty), \end{aligned}\right\} \tag{12}$$

on the real line. The techniques which must be used because neither $y(t)$ or $\beta(t)$ are known initially will be discussed later.

The general solution of the Riemann–Hilbert mixed boundary-value problem in an upper half-plane is well known (e.g. Larock & Street 1965). If the imaginary part of some function $Q(t)$, $\mathrm{Im}\,[Q(t)]$, is known at all points on the real line, then the solution is

$$Q(t) = \frac{1}{\pi}\int_{-\infty}^{\infty} \frac{\mathrm{Im}\,[Q(\eta)]}{\eta - t} d\eta + \Sigma A_j t^j, \tag{13}$$

which is a regular analytic function in the entire upper half-plane. If the quotient $Q(t) = \omega(t)/H(t)$ can be constructed in such a way that $\mathrm{Im}\,[Q(t)]$ is known on the real line, as required, then the Riemann–Hilbert solution can be used to construct $\omega(t)$ explicitly. Following the method of Cheng & Rott (1954), the solution to the homogeneous analogue of (12) is introduced (Larock 1969*a*) as

$$H(t) = [t(1+t)]^{\frac{1}{2}}. \tag{14}$$

The requirements that the flow separate smoothly at B and be uniform at D forces $A_j = 0$ for all j (Larock 1969*a*). Formally the expression for $\omega(t)$ is therefore

$$\frac{\omega(t)}{H(t)} = \frac{1}{2\pi}\int_{-1}^{0} \frac{\ln\left[1-\frac{2}{F^2}\left(\frac{y(\eta)}{y_2}-1\right)\right]d\eta}{(\eta-t)\left[-\eta(1+\eta)\right]^{\frac{1}{2}}} + \frac{1}{\pi}\int_{0}^{t_A} \frac{\beta(\eta)\,d\eta}{(\eta-t)\left[\eta(1+\eta)\right]^{\frac{1}{2}}}. \tag{15}$$

The parameter t_A is determined by requiring that $q = q_1$ and $\theta = 0$ far upstream at $D(t \to \infty)$. This is equivalent to requiring that

$$\ln\left(\frac{q_1}{q_2}\right) = -\ln\left(\frac{y_1}{y_2}\right) = \frac{1}{2\pi}\int_{-1}^{0} \frac{\ln\left[1-\frac{2}{F^2}\left(\frac{y(\eta)}{y_2}-1\right)\right]d\eta}{\left[-\eta(1+\eta)\right]^{\frac{1}{2}}} - \int_{0}^{t_A} \frac{\beta(\eta)\,d\eta}{\left[\eta(1+\eta)\right]^{\frac{1}{2}}} \tag{16}$$

be satisfied. Now $\omega(t)$ is known, and the resulting configuration in the physical plane is given by (11). Furthermore, if the local pressure coefficient

$$C_p = p/(\tfrac{1}{2}\rho q_2^2) \tag{17}$$

is wanted at any point in the flow, (2), (6) and (7) give C_p in terms of ω and its conjugate $\bar{\omega}$ as

$$C_p = 1 - \exp(\omega + \bar{\omega}). \tag{18}$$

3. The gate curvature function $\beta(t)$

Ideally the local gate inclination β would be directly prescribed as a function of z. This goal is not attainable for the current problem, however, because of the inverse nature of the solution. Instead it is required that β be described as a known function of t. Larock (1969*b*) has shown that any piecewise continuous polynomial representation of $\beta(t)$ can be rather easily incorporated into the current theory, although higher order expressions for $\beta(t)$ can quickly produce bulky results. Fortunately it was found that a prescribed linear variation for $\beta(t)$ produces nearly circular arcs in the physical plane. It was further found that a simple linear variation in $\beta(t)$ was not nearly so successful in producing an approximately constant radius of curvature R as was a prescription of two separate linear variations in $\beta(t)$ over the ranges $(0, t_J)$ and (t_J, t_A) between points A and B. At the juncture point t_J (point J in figure 1) $\beta(t)$ was required to be continuous but $\beta'(t)$ was allowed to have a discontinuity. With this prescription for $\beta(t)$ it was possible to keep the local radius of curvature R from varying by more than 1–3 %, with the larger value applying only to those gates with a larger included angle between A and B.

Mathematically, $\beta(t)$ was constructed to satisfy the requirements that

$$\left.\begin{aligned} \beta &= \beta_1 \quad \text{at} \quad t = t_A, \\ \beta &= \beta_2 \quad \text{at} \quad t = t_J, \\ \beta &= \beta_3 \quad \text{at} \quad t = 0, \end{aligned}\right\} \tag{19}$$

with linear variation at intermediate t points. Hence, $\beta(t)$ is given as

$$\left.\begin{aligned} \beta(t) &= \beta_3 + (\beta_2 - \beta_3)\,t/t_J \qquad (0 \leqslant t \leqslant t_J), \\ \beta(t) &= [(\beta_1 - \beta_2)t + \beta_2 t_A - \beta_3 t_J]/(t_A - t_J) \quad (t_J \leqslant t \leqslant t_A). \end{aligned}\right\} \tag{20}$$

It was felt that this choice represented a judicious balance between mathematical simplicity and accuracy of physical representation.

4. The solution

The results of this study are primarily a knowledge of the relation between gate geometry, the contraction coefficient C_c and discharge coefficient C_d for the gate and the downstream free-surface location. Also determined in the study was the variation in fluid speed and pressure coefficient on the gate and along the channel bottom under the gate. Letting

$$G_D = -\frac{1}{2}\int_{-1}^{0} \frac{\ln\left[1-\frac{2}{F^2}\left(\frac{y(\eta)}{y_2}-1\right)\right]d\eta}{[-\eta(1+\eta)]^{\frac{1}{2}}}, \tag{21}$$

the substitution of (20) for $\beta(t)$ into (16) gives

$$\begin{aligned}\pi \ln\left(\frac{y_1}{y_2}\right) = G_D &+ \frac{\beta_2-\beta_3}{t_J}[t_J(1+t_J)]^{\frac{1}{2}} + \left[\beta_3 - \left(\frac{\beta_2-\beta_3}{2t_J}\right)\right]\ln\{2t_J+1+2[t_J(1+t_J)]^{\frac{1}{2}}\} \\ &+ \frac{\beta_1-\beta_2}{t_A-t_J}\left\{[t_A(1+t_A)]^{\frac{1}{2}} - [t_J(1+t_J)]^{\frac{1}{2}} - \tfrac{1}{2}\ln\left[\frac{2t_A+1+2[t_A(1+t_A)]^{\frac{1}{2}}}{2t_J+1+2[t_J(1+t_J)]^{\frac{1}{2}}}\right]\right\} \\ &+ \left(\frac{1}{t_A-t_J}\right)(\beta_2 t_A - \beta_1 t_J)\ln\left[\frac{2t_A+1+2[t_A(1+t_A)]^{\frac{1}{2}}}{2t_J+1+2[t_J(1+t_J)]^{\frac{1}{2}}}\right]\end{aligned} \tag{22}$$

as the condition which fixes t_A. In satisfying this equation the ratio $\lambda = t_J/t_A$, essentially a shape factor for the gate, was normally fixed. Then the computer employed a successive approximation procedure, actually a bisection process, to find a root t_A which satisfied (22).

The complete expression for $\omega(t)$, upon insertion of (20) into (15), is

$$\begin{aligned}\frac{\omega(t)}{H(t)} = -\frac{1}{2\pi}\int_{-1}^{0} &\frac{\ln\left[1-\frac{2}{F^2}\left(\frac{y(\eta)}{y_2}-1\right)\right]d\eta}{(\eta-t)[-\eta(1+\eta)]^{\frac{1}{2}}} + \frac{\beta_2-\beta_3}{\pi t_J}\int_0^{t_J}\frac{d\eta}{[\eta(1+\eta)]^{\frac{1}{2}}} \\ &+ \frac{\beta_1-\beta_2}{\pi(t_A-t_J)}\int_{t_J}^{t_A}\frac{d\eta}{[\eta(1+\eta)]^{\frac{1}{2}}} + \frac{1}{\pi t_J}[(\beta_2-\beta_3)t+\beta_3 t_J]\int_0^{t_J}\frac{d\eta}{(\eta-t)[\eta(1+\eta)]^{\frac{1}{2}}} \\ &+ \frac{1}{\pi(t_A-t_J)}[(\beta_1-\beta_2)t+\beta_2 t_A-\beta_1 t_J]\int_{t_J}^{t_A}\frac{d\eta}{(\eta-t)[\eta(1+\eta)]^{\frac{1}{2}}}.\end{aligned} \tag{23}$$

By defining the quantities

$$G_p(t) = -\frac{1}{2\pi}[t(1+t)]^{\frac{1}{2}}\int_{-1}^{0}\frac{\ln\left[1-\frac{2}{F^2}\left(\frac{y(\eta)}{y_2}-1\right)\right]d\eta}{(\eta-t)[-\eta(1+\eta)]^{\frac{1}{2}}}, \tag{24a}$$

for $0 \leqslant t \leqslant t_A$, and

$$G_s(t) = -\frac{1}{2\pi}[-t(1+t)]^{\frac{1}{2}}\int\!\!\!\!\!\!-_{-1}^{0}\frac{\ln\left[1-\frac{2}{F^2}\left(\frac{y(\eta)}{y_2}-1\right)\right]d\eta}{(\eta-t)[-\eta(1+\eta)]^{\frac{1}{2}}}, \tag{24b}$$

for $-1 < t < 0$, where the slash on the integral sign indicates the deletion of the point $\eta = t$ from the range of integration, the substitution of (20) into (15) gives $\omega(t)$ along the gate as

$$\omega(t) = i\beta(t) + G_p(t) + M(t) \quad (0 \leqslant t \leqslant t_A), \tag{25}$$

and along the downstream free surface as

$$\omega(t) = iG_s(t) - iB(t) + \tfrac{1}{2}\ln\left[1 - \frac{2}{F^2}\left(\frac{y(t)}{y_2} - 1\right)\right] \quad (-1 \leqslant t \leqslant 0). \tag{26}$$

Introduced above is the notation

$$M(t) = \sum_{k=1}^{3} M_k(t), \tag{27a}$$

$$M_1(t) = \left\{\left(\frac{\beta_2 - \beta_3}{t_J}\right)\ln\left[2t_J + 1 + 2[t_J(1+t_J)]^{\frac{1}{2}}\right] + \left(\frac{\beta_1 - \beta_2}{t_A - t_J}\right)\ln\left[\frac{2t_A + 1 + 2[t_A(1+t_A)]^{\frac{1}{2}}}{2t_J + 1 + 2[t_J(1+t_J)]^{\frac{1}{2}}}\right]\right\}[t(1+t)]^{\frac{1}{2}}, \tag{27b}$$

$$M_2(t) = -\frac{1}{\pi}\left[(\beta_2 - \beta_3)\frac{t}{t_J} + \beta_3\right]\ln\left|\frac{2[tt_J(1+t)\,(1+t_J)]^{\frac{1}{2}} + t + t_J + 2tt_J}{t - t_J}\right|, \tag{27c}$$

$$M_3(t) = -\frac{1}{\pi}\left(\frac{1}{t_A - t_J}\right)[(\beta_1 - \beta_2)t + \beta_2 t_A - \beta_1 t_J] \times \ln\left|\left(\frac{2[tt_A(1+t)\,(1+t_A)]^{\frac{1}{2}} + t + t_A + 2tt_A}{2[tt_J(1+t)\,(1+t_J)]^{\frac{1}{2}} + t + t_J + 2tt_J}\right)\left(\frac{t - t_J}{t - t_A}\right)\right|, \tag{27d}$$

and

$$B(t) = -\sum_{k=1}^{3} B_k(t), \tag{28a}$$

$$B_1(t) = \frac{1}{\pi}\left\{\left(\frac{\beta_2 - \beta_3}{t_J}\right)\ln\left[2t_J + 1 + 2[t_J(1+t_J)]^{\frac{1}{2}}\right] + \left(\frac{\beta_1 - \beta_2}{t_A - t_J}\right)\ln\left[\frac{2t_A + 1 + 2[t_A(1+t_A)]^{\frac{1}{2}}}{2t_J + 1 + 2[t_J(1+t_J)]^{\frac{1}{2}}}\right]\right\}[-t(1+t)]^{\frac{1}{2}}, \tag{28b}$$

$$B_2(t) = \frac{1}{\pi}\left[(\beta_2 - \beta_3)\frac{t}{t_J} + \beta_3\right]\left\{\sin^{-1}\left[1 + 2t + \frac{2t(1+t)}{t_J - t}\right] + \frac{\pi}{2}\right\}, \tag{28c}$$

$$B_3(t) = \frac{1}{\pi}\left(\frac{1}{t_A - t_J}\right)[(\beta_1 - \beta_2)t + \beta_2 t_A - \beta_1 t_J] \times \left\{\sin^{-1}\left[1 + 2t + \frac{2t(1+t)}{t_A - t}\right] - \sin^{-1}\left[1 + 2t + \frac{2t(1+t)}{t_J - t}\right]\right\}. \tag{28d}$$

It should be noted that

$$G_p(0) = \tfrac{1}{2}\ln\left[1 - \frac{2}{F^2}\left(\frac{y_B}{y_2} - 1\right)\right] \tag{29}$$

and $G_s(0) = G_s(-1) = 0$ where y_B is the y co-ordinate of the gate lip, point B.

The gate shape is then given parametrically by (8) in the form

$$\frac{x(t) - x_0}{y_2} = -\frac{1}{\pi}\int_{t_0}^{t}\frac{\exp[-M(\eta)]\cos\beta(\eta)\,d\eta}{1+\eta}, \tag{30a}$$

and

$$\frac{y(t) - y_0}{y_2} = \frac{1}{\pi}\int_{t_0}^{t}\frac{\exp[-M(\eta)]\sin\beta(\eta)\,d\eta}{1+\eta}. \tag{30b}$$

If one integrates from the known point A towards point B, then $t_0 = t_A$, $t < t_A$, $x_0 = 0$ and $y_0 = y_1$. Along the gate the local pressure coefficient C_p is simply given by (18) as

$$C_p = 1 - \exp[2M(t)] \quad (0 < t < t_A). \tag{31}$$

The shape of the downstream free surface is given by combining (8) and (23) to obtain another pair of parametric expressions:

$$\frac{x(t)-x_0}{y_2} = -\frac{1}{\pi}\int_{t_0}^{t} \frac{\cos\left[B(\eta)-G_s(\eta)\right]d\eta}{(1+\eta)\left[1-\frac{2}{F^2}\left(\frac{y(\eta)}{y_2}-1\right)\right]^{\frac{1}{2}}}, \tag{32a}$$

$$\frac{y(t)-y_0}{y_2} = -\frac{1}{\pi}\int_{t_0}^{t} \frac{\sin\left[B(\eta)-G_s(\eta)\right]d\eta}{(1+\eta)\left[1-\frac{2}{F^2}\left(\frac{y(\eta)}{y_2}-1\right)\right]^{\frac{1}{2}}}. \tag{32b}$$

To begin integration from the gate lip, point B, one selects

$$t_0 = 0, \quad t < 0, \quad x_0 = x_B = x(0) \quad \text{and} \quad y_0 = y_B = y(0).$$

The contraction coefficient and discharge coefficient for the gate can now be readily determined. The contraction coefficient C_c is the ratio of the downstream depth to the gate opening, or $C_c = y_2/y_B$. The discharge per unit width Q_d is related to the product of the gate width y_B and a convenient reference velocity $(2gy_1)^{\frac{1}{2}}$ by the discharge coefficient C_d; i.e.

$$Q_d = C_d y_B (2gy_1)^{\frac{1}{2}}. \tag{33}$$

Using this definition in conjunction with (1) and (2) gives

$$C_d = \frac{C_c}{[1+C_c y_B/y_1]^{\frac{1}{2}}}. \tag{34}$$

The solution to this problem can be and has been extended to the determination of velocities and pressures along the channel bottom as well as on the gate itself; some of these results will be presented graphically in the next section. Only the method of performing these computations will be outlined here, however, for it is felt that these results will not be so useful as the relations already presented. Equation (23) can easily be evaluated for $t < -1$, and then (7) and (8) yield rather easily the local velocity and the z plane co-ordinate for each value of t. By extending the centre portion of (2) to include a local pressure term, the gauge pressure p at any interior point in the flow is found to be

$$\frac{p}{\frac{1}{2}\rho q_2^2} = 1-\left(\frac{q}{q_2}\right)^2+\frac{2}{F^2}\left(1-\frac{y}{y_2}\right). \tag{35}$$

Of course, on the channel bottom $y = 0$. Establishing a relation between a known free-surface point z_s and a point on the channel floor z_f is conceptually straightforward but is also algebraically tedious. The correspondence is obtained by integrating (8) along the arc $t = -1+\delta e^{i\nu}$ ($\delta \ll 1, 0 \leqslant \nu \leqslant \pi$) to avoid the singularity at $t = -1$. One substitutes this relation into (8), rearranges the resulting massive expression into real and imaginary parts and evaluates the final quadratures on the computer.

5. Results and computing procedures

Figure 4 depicts a radial gate with four different depths of flow upstream shown. Or the figure may be interpreted as showing four closely related but geometrically distinct radial gates, each having a different flow depth, although it was the

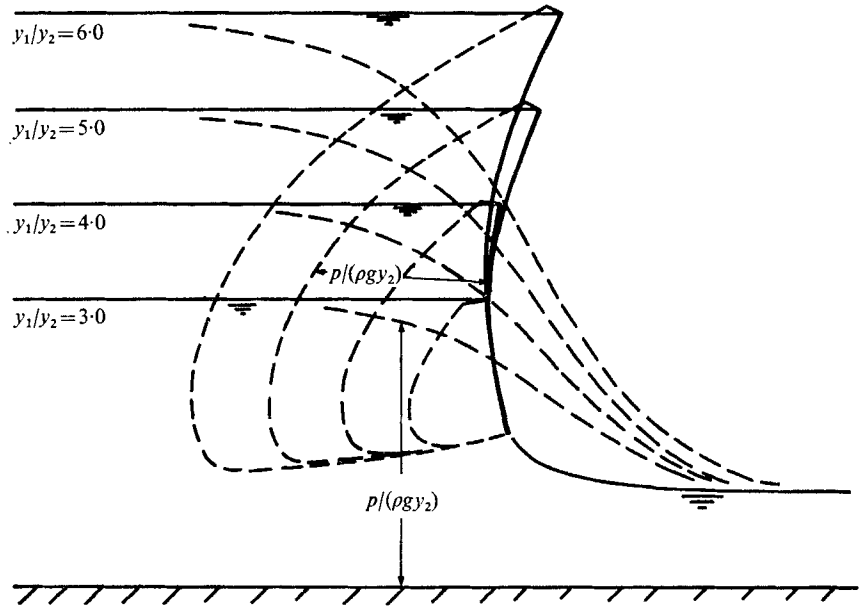

FIGURE 4. The radial gate and pressure distributions $p/(\rho g y_2)$.

y_1/y_2	b/y_2	a/y_2	$\bar{R}/y_2$	C_c	b/y_1	F^2
6·0	1·594	3·297	6·53	0·6275	0·2656	10·29
5·0	1·602	3·005	5·37	0·6242	0·3204	8·33
4·0	1·610	3·104	5·76	0·6209	0·4027	6·40
3·0	1·614	3·355	6·79	0·6195	0·5381	4·50

TABLE 1. Computed parameters for radial gate, figure 4

y_1/y_2	β_1	β_2 degrees	β_3	$\lambda = t_J/t_A$	t_A	G_D	δ_R %
6·0	115·0	95·0	75·0	0·70	11·27	0·12	3·1
5·0	112·2	93·6	74·9	0·71	7·27	0·15	2·5
4·0	99·0	87·0	75·0	0·68	4·41	0·21	0·9
3·0	87·0	81·0	74·8	0·68	2·08	0·30	0·2

TABLE 2. Additional parameters for radial gate, figure 4

writer's intent to study one gate as an example. Since the physical-plane configuration is itself a computed result, it is not easily controlled in a precise manner. On the other hand, a gate shape which is reasonably close to a specified shape is not difficult to obtain. Tables 1 and 2 give the value of various gate and flow parameters for the flows of figure 4.

In the example y_1/y_2 and the curvature function $\beta(t)$ were specified. Although the lip inclination was $\beta_3 = 75°$ for each depth, the contraction coefficient C_c decreased slightly as the upstream depth decreased. The variation in trunnion elevation a and mean radius of curvature $\bar{R}$ is a further result of the inverse nature of the solution. After a solution was computed, the location of the trunnion or pivot for the gate was found by computing the intersection point of lines drawn perpendicularly through points A and B. The distance to point J was then found. Calling the distances from points A, B and J to the pivot R_A, R_B and R_J respectively, $\bar{R} = \frac{1}{3}(R_A + R_B + R_J)$. Since it was noted that small values of F^2 indicated a significant gravity effect, F^2 is also tabulated. For values of y_1/y_2 much less than 3·0, it is felt that the current flow model with its horizontal upstream upper surface is probably unrealistic and should not be used.

Table 2 gives additional parameters associated with the example. As pointed out earlier, neither $y(t)$ nor $\beta(t)$ is initially known for a given gate geometry. Because of the choice of flow model, a fluid flow still exists past the gate in the absence of gravity. Furthermore, the computer program for this problem executes in a few seconds in the absence of gravity. Values of y_1/y_2, β_1, β_2 and β_3 would be prescribed from physical considerations, and non-gravity trial cases were computed for several prescribed values of $\lambda = t_J/t_A$; the λ-value that minimized the variation in $\bar{R}$ was chosen for use in the subsequent gravity computations. The non-gravity solution also computed a free-surface location $y(t)$ which could be used as a first approximation in an iterative process to find the solution for the gravity-affected flow.

Iteration to find the gravity solution now began. It was desired not to change t_A or λ in satisfying (22), for altering these basic t plane parameters would affect the entire solution in a non-linear fashion. However, β_3 can easily be adjusted to satisfy (22) since the equation is linear in β_3. Thus G_D was computed and β_3 was adjusted. Using $y(t)$ from the previous iteration, arrays of values for $G_p(t)$ and $G_s(t)$ were computed, and then the complete solution was computed. This iterative cycle was repeated until the solution converged, usually after 2 or 3 cycles. Table 3 shows the rate of convergence of several key parameters for the case $y_1/y_2 = 4{\cdot}0$, which is rather strongly influenced by gravity. Cycle 0 is the non-gravity solution which starts with $G_D = 0{\cdot}0$. Two or three trials are needed to select β_3 so that, after adjustments, one later achieves the desired final value for it. During the solution β_3 always decreased from one iteration to the next. Apparently 2 cycles of this solution would have been adequate for most purposes. For each case table 2 gives the final value of G_D which, like F^2, is a good measure of the effect of gravity on the flow. As a measure of the constancy of the gate radius of curvature, the maximum range of $R/\bar{R}$ along the gate is noted and expressed as a percentage δ_R.

Figure 4 also shows computed pressure distributions along both the gate and channel bottom. The quantity $p/(\rho g y_2)$ is plotted normally from the gate surface and vertically along the channel bottom. The form of this plot compares well with Metzler's (1948) experimental work. Due to the parameterization of this solution, however, it was not possible to produce easily a set of data which could be directly compared with his results.

Figure 5 compares the contraction coefficients C_c for the radial gate (table 1) with C_c for a planar gate, each having a lip inclination $\beta_3 = 75°$. As $b/y_1 \to 0$ (or as $y_1 \to \infty$), $C_c \to 0{\cdot}647$ according to classical theory. For finite curvature the radial gate C_c is definitely below the planar gate C_c but not markedly so. The small difference clearly occurs because most of the radial gate is locally inclined more steeply than 75°.

Cycle	β_3 (degrees)	C_c	b/y_1	G_D
0	81·14	0·6449	0·3877	0·0
1	75·72	0·6237	0·4008	0·1814
2	75·09	0·6212	0·4024	0·2024
3	75·01	0·6209	0·4027	0·2051
4	75·00	0·6209	0·4027	0·2055

TABLE 3. Rate of convergence of parameters for the case $y_1/y_2 = 4{\cdot}0$, figure 4

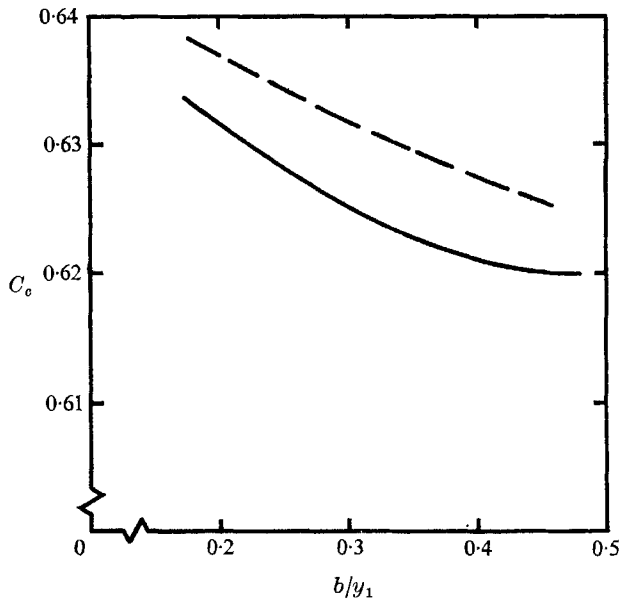

FIGURE 5. Comparison of C_c for radial gate and planar gate with lip inclination $\beta_3 = 75°$. ———, radial gate; – – –, planar gate.

Information on radial gate performance is often summarized in data on the discharge coefficient C_d as a function of gate geometry. In table 4 some results of the current theory are compared to data from other sources. Toch (1955) performed a relatively complete set of experiments to determine $C_d(y_1/R, b/R, a/R)$ for both the free and submerged outflow cases. His reported results were restricted to $a/R = 0{\cdot}1$, 0·5, 0·9. An enlarged copy of his summary plot is found in Henderson (1966). The U.S. Army Engineer Waterways Experiment Station (WES) has prepared (1960) hydraulic design charts based on data from several sources, including Toch. Design curves were interpolated between data points.

WES remarks that values from the chart seem to conform to experimental results to within $\pm 3\%$. Babb (1966) supervised an extensive experimental program to determine discharge coefficients from the radial gates used in the California Aqueduct; logarithmic fitting techniques were used to obtain reasonably accurate mathematical expressions for the discharge coefficient. This was done, and the investigators found an average error of about 3 % between the equations and individual experiments. Since Babb's results are applicable only to a particular gate configuration, they cannot be used to check other results.

	Discharge coefficient C_d				
Source	Case... 1	2	3	4	5
Larock	0·581	0·570	0·555	0·537	0·648
Toch	0·56	0·54	0·53	0·51	0·63–0·64
WES	0·567	0·555	0·543	0·528	0·645
Babb	—	—	—	—	0·667

TABLE 4. Comparison of discharge coefficients C_d from several sources

In table 4 the columns labelled as cases 1–4 report the results from figure 4 and tables 1 and 2; case 1 corresponds to $y_1/y_2 = 6{\cdot}0$ and cases 2–4 correspond to $y_1/y_2 = 5{\cdot}0$, $4{\cdot}0$, and $3{\cdot}0$, respectively. Case 5 closely reproduces one flow past the California Aqueduct radial gate. The current theory correlates best with the WES design charts and less well with Toch. The differences between WES and the theoretical predictions are in the same direction and approximately of the same magnitude as Fangmeier & Strelkoff (1968) report in a comparison between theory and experiment for the vertical sluice gate. The fact that Toch's plots are quite small makes it difficult to read the graphs accurately and may contribute to the apparent inaccuracies. In almost every case a 3–5 % change in the result would bring theory and experiment into agreement.

It is natural to inquire what must be done to improve further the agreement between theory and experiment. A comparison of the vertical sluice gate study by Fangmeier & Strelkoff (1968) and the planar gate study by the writer (Larock 1969*a*) indicates that the presence of the horizontal upstream surface in the current study causes the theory to predict contraction coefficients which are slightly high. This difference does not noticeably affect computed discharge coefficients, however. One also expects the viscosity of the real fluid to cause small but significant deviations between theory and experiment; Benjamin (1956) and several more recent writers have shown that consideration of a laminar boundary layer forming along the channel bottom beneath the gate properly explains the order of magnitude of the difference between theory and experiment for C_c. For this reason boundary-layer corrections were considered briefly in the current study. In computing pressures in this study, local velocities were first calculated. Velocities were quite low over most of the gate, and most of the velocity change along the channel bottom occurred in a distance $\pm y_1$ from the gate. Thus it was felt that boundary-layer formation on the gate could be ignored. Along the channel bottom Thwaites's method (Rosenhead 1963) of computing a laminar

boundary layer in a favourable pressure gradient was applied to determine the displacement thickness as a function of distance along the channel bottom. As a result it appears that a simple displacement thickness approach to the viscous correction factor for the problem is not quantitatively sufficient. A more complete study seems to be needed.

Conformal mapping and the Riemann–Hilbert solution to a mixed boundary-value problem form the basis of a rapidly convergent, iterative technique which describes the free outflow from radial gates. Relatively good agreement with a limited number of experimental results was shown. Circumstances permitting, it would be desirable to compute a larger number of cases so that (i) theory and experiment might be checked more thoroughly and (ii) some useful engineering design charts might be plotted on the basis of the theory. The limited results indicate, however, that the theory can produce sufficiently accurate results for use in many engineering projects.

REFERENCES

Babb, A., Moayeri, M. & Amorocho, J. 1966 Discharge coefficients of radial gates. *University of California, Davis, Water Science and Engineering Paper* **1013.**

Benjamin, T. B. 1956 On the flow in channels when rigid obstacles are placed in the stream. *J. Fluid Mech.* **1**, 227.

Cheng, H. K. & Rott, N. 1954 Generalizations of the inversion formula of thin airfoil theory. *J. Rat. Mech. Anal.* **3**, 357.

Churchill, R. B. 1960 *Complex Variables and Applications* (2nd edn.). New York: McGraw-Hill.

Fangmeier, D. D. & Strelkoff, T. S. 1968 Solution for gravity flow under a sluice gate. *J. Engng Mech. Div., Am. Soc. Civ. Engrs*, **94**, 153.

Henderson, F. M. 1966 *Open Channel Flow.* New York: Macmillan.

Klassen, V. J. 1967 Flow from a sluice gate under gravity. *J. Math. Analysis Applic.* **19**, 253.

Larock, B. E. 1969*a* Gravity-affected flow from planar sluice gates. *J. Hydraul. Div. Am. Soc. Civ. Engrs*, **95**, 1211.

Larock, B. E. 1969*b* Jets from two-dimensional symmetric nozzles of arbitrary shape. *J. Fluid Mech.* **37**, 479.

Larock, B. E. & Street, R. L. 1965 A Riemann–Hilbert problem for non-linear, fully cavitating flow. *J. Ship Res.* **9**, 170.

Larock, B. E. & Street, R. L. 1967 A nonlinear theory for a fully cavitating hydrofoil in a transverse gravity field. *J. Fluid Mech.* **29**, 317.

Metzler, D. E. 1948 A model study of Tainter-gate operation. M.S. Thesis, State University of Iowa.

Pajer, G. 1937 Über den Stromungsvorgang an einer unterstromten scharfkantigen Planschutze. *Z. angew. Math. Mech.* **17**, 259.

Perry, B. 1957 Methods for calculating the effect of gravity on two-dimensional free surface flows. Ph.D. Thesis, Stanford University.

Rayleigh, Lord 1876 Notes on hydrodynamics. *Phil. Mag.* (5) **2**, 441.

Rosenhead, L. 1963 *Laminar Boundary Layers.* Oxford University Press.

Southwell, R. B. & Vaisey, G. 1946 Relaxation methods applied to engineering problems. 12. Fluid motions characterized by 'free' streamlines. *Phil. Trans.* A **240**, 117.

Toch, A. 1955 Discharge characteristics of Tainter gates. *Trans. Am. Soc. Civ. Engrs*, **120**, 290.

Von Mises, R. 1917 Berechnung von Ausfluss-und Überfallzahlen. *Z. Ver. dt. Ing.* **61**, 447, 469, 493.